

10.6% Certified Colloidal Quantum Dot Solar Cells via Solvent-Polarity-Engineered Halide Passivation

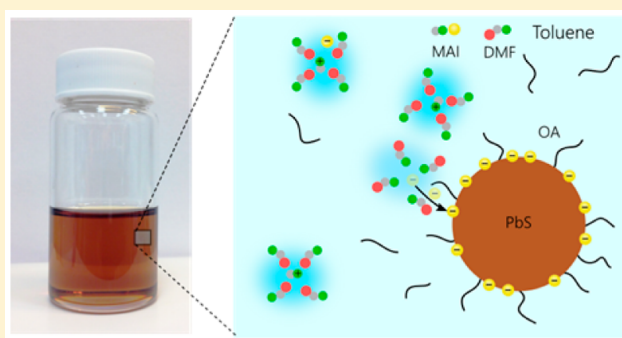
Xinzheng Lan, Oleksandr Voznyy, F. Pelayo García de Arquer, Mengxia Liu, Jixian Xu, Andrew H. Proppe, Grant Walters, Fengjia Fan, Hairen Tan, Min Liu, Zhenyu Yang, Sjoerd Hoogland, and Edward H. Sargent*

Department of Electrical and Computer Engineering, University of Toronto, 10 King's College Road, Toronto, Ontario M5S 3G4, Canada

S Supporting Information

ABSTRACT: Colloidal quantum dot (CQD) solar cells are solution-processed photovoltaics with broad spectral absorption tunability. Major advances in their efficiency have been made via improved CQD surface passivation and device architectures with enhanced charge carrier collection. Herein, we demonstrate a new strategy to improve further the passivation of CQDs starting from the solution phase. A cosolvent system is employed to tune the solvent polarity in order to achieve the solvation of methylammonium iodide (MAI) and the dispersion of hydrophobic PbS CQDs simultaneously in a homogeneous phase, otherwise not achieved in a single solvent. This process enables MAI to access the CQDs to confer improved passivation. This, in turn, allows for efficient charge extraction from a thicker photoactive layer device, leading to a certified solar cell power conversion efficiency of 10.6%, a new certified record in CQD photovoltaics.

KEYWORDS: PbS quantum dots, solar cells, solvent polarity, passivation, methylammonium iodide



Solar cells based on PbX (X = S, Se) colloidal quantum dots (CQDs) have advanced in the past decade as a result of worldwide research efforts.^{1–6} Their broad spectral response, solution-processing, and air stability promise low-cost high efficiency photovoltaics.^{6–11}

For a typical colloidal synthesis, long-chain organic-ligand-stabilized CQDs can be prepared with controlled size and excellent monodispersity, each of which is crucial for photovoltaic applications.^{12–16} To build a high-quality photovoltaic QD solid, interdot electronic communication needs to be improved, since the bulky organic ligands that afford CQDs' colloidal stability otherwise create electronic barriers that compromise efficient charge transport. Exchange to shorter ligands either in solution or in film has been widely employed: through these exchanges, carrier mobility has been enhanced by several orders of magnitude.^{17–23}

The inherent large surface-to-volume ratio of QD materials results in unsaturated dangling bonds, creating undesired electronic trap states within the bandgap of QD solids. The ligand exchange procedure itself is prone to create new, rather than passivate existing, dangling bonds. These trap states increase the chance of carrier recombination, curtailing the efficiency of charge extraction. For this reason, a series of strategies have been developed to passivate trap states at each step in processing, such as organic–inorganic hybrid

passivation, atomic passivation, and perovskite–matrix passivation.^{2,9,24–27}

Atomic halide ligands have attracted the most attention among the various passivation schemes thanks to their strong passivation and the air-stability of the resulting QD solids afforded by strong Pb–Y (Y = Cl, Br, and I) binding.^{28–30} Recently, we have demonstrated the use of molecular iodine pretreatment in solution to improve surface passivation. This translated into an increased diffusion length in a solar cell device and allowed for an increased thickness of the active layer without compromising charge extraction. With this approach, a certified record efficiency of 9.9% was demonstrated.⁶ Unfortunately, the highly reactive nature of molecular iodine can lead to uncontrolled fusion of PbS CQDs. The high surface energy of PbS CQDs (~3 nm in diameter) and the loss of ligands during the treatment may be responsible for the fusion process.

Here we sought to introduce more iodine on the CQD surface without the detrimental effect of fusion. We achieved this by treating the CQDs with a much milder iodine source, methylammonium iodide (MAI). We employed a cosolvent

Received: May 13, 2016

Revised: June 24, 2016

system to tune the solvent polarity in order to achieve the solvation of MAI and the dispersion of hydrophobic PbS CQDs simultaneously in a homogeneous phase. We find that this otherwise cannot be achieved in a single solvent. This enables MAI to access the PbS CQDs to confer improved passivation. At the same time, an additional ion-pair ligand shell helps to avoid the fusion of PbS CQDs. As a consequence, when CQD films were assembled into solar cell devices, a certified efficiency of 10.6% was achieved, a new record efficiency in certified CQD photovoltaics.

We illustrate the MAI treatment process in Figure 1.³¹ A highly polar solvent is required for the solvation of the ionic-

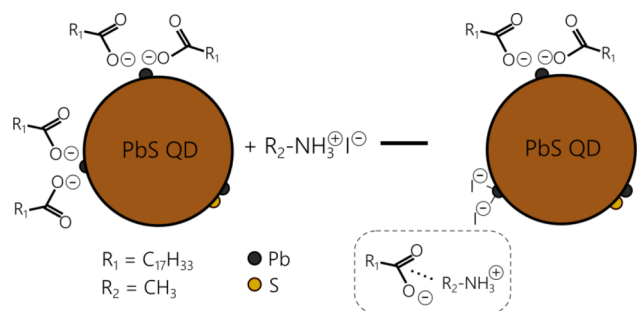


Figure 1. Ligand shell changes following MAI treatment. DMF-solvated Γ^- ligands partially replace long-chain oleate ligands on the CQD surface. An additional shell of $\text{MA}^+\text{-OAc}^-$ ion pairs is formed as a result of the electrostatic attraction, thereby offering steric hindrance in addition to tightly bound oleates remaining on the surface.

bond-stabilized MAI, whereas nonpolar solvents are needed to disperse oleic acid (OA)-capped PbS CQDs. In order to enable MAI to access the CQDs in solution, we develop a cosolvent strategy that employs a mixture of two miscible solvents, toluene and dimethylformamide (DMF), to tune the solvent polarity. As a result, this cosolvent system results in the simultaneous dispersion of MAI and PbS CQDs. The DMF-solvated Γ^- anions will react with OA-capped PbS QDs, thereby enabling the incorporation of Γ^- ligands prior to the film assembly process. The ligand exchange process in the MAI treatment is described by the equation $\text{PbS}[\text{Pb}(\text{OA})_2] + 2 \text{MA}^+\Gamma^- \rightarrow \text{PbS}(\text{PbI}_2) + 2 \text{MA}^+\text{OAc}^-$. We hypothesize that, during this ligand exchange process, an additional ligand shell of $\text{MA}^+\text{-OAc}^-$ ion pairs will form as a result of electrostatic attraction, thereby offering further hindrance to fusion among CQDs.^{32,33} We used ^1H NMR spectroscopy to monitor the ligand exchange process. Before the MAI treatment, a broad alkene resonance centered at 5.8 ppm arises from the surface-bound OA (Figure S1).³¹ After the MAI treatment, a new peak appears, consistent with the detachment of OA and, possibly, formation of a dynamically interacting ligand shell (Figures S2 and S3).

Figure 2a shows the spectral absorbance of PbS CQDs in solution before and after the MAI treatment. The excitonic peak remains well-preserved following the treatment. Photoluminescence (PL) analysis further suggests that the CQD size and monodispersity are kept intact (Figure 2b). High-resolution transmission electron microscopy (HRTEM) analysis supports the view that no fusion occurred after the

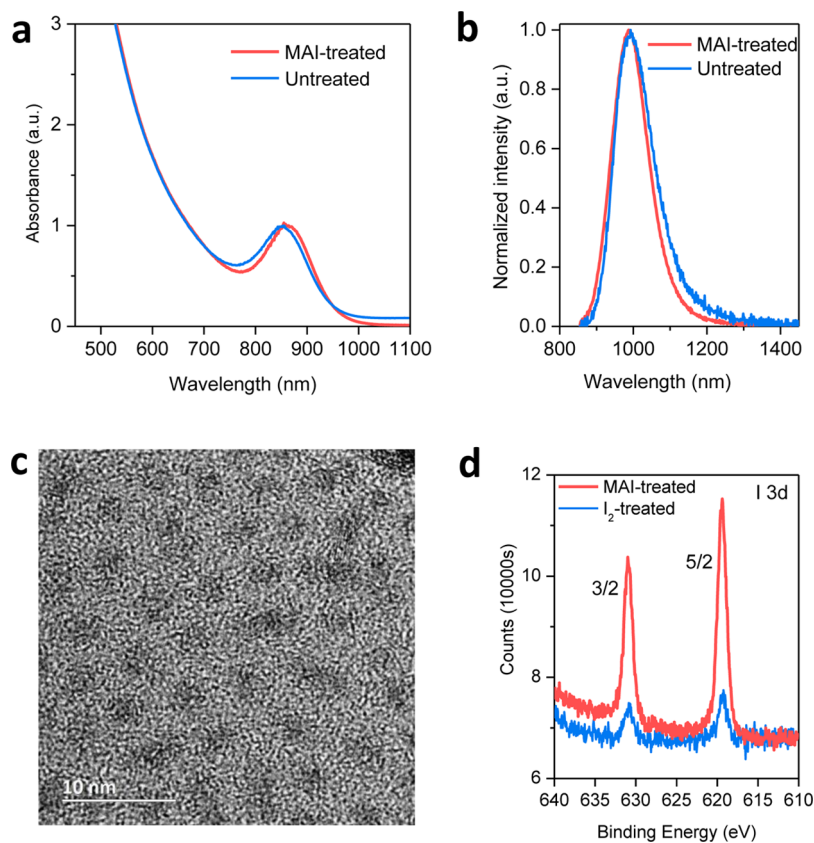


Figure 2. Characterization of CQDs following different treatments. Absorption (a) and (b) photoluminescence spectra of CQDs before and after MAI treatment. (c) HRTEM image of MAI-treated CQDs, suggesting no fusion. (d) I 3d peak of both I_2 -treated and MAI-treated CQDs, demonstrating greatly enhanced I-incorporation for the MAI case.

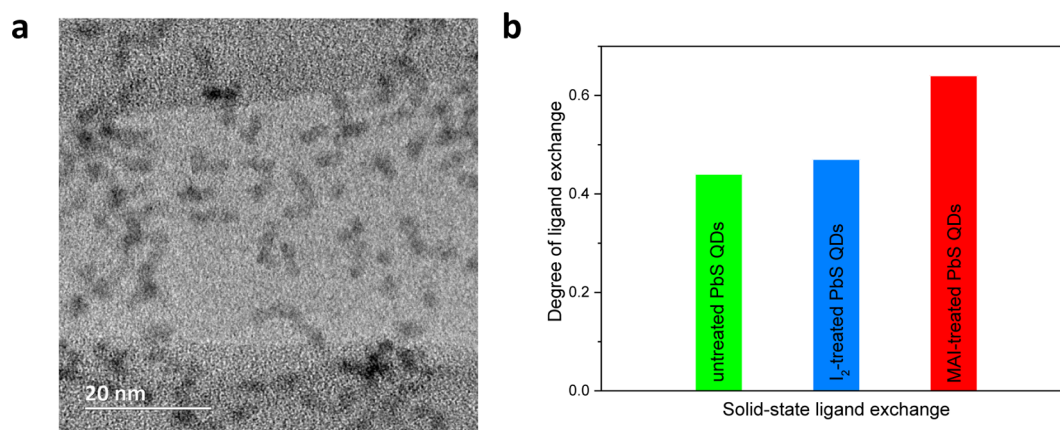


Figure 3. (a) HRTEM image of two-week aged MAI-treated PbS CQDs following methanol washing. (b) Compositional analysis of TBAI-exchange PbS active layer for both un-, I_2 -, and MAI-pretreated PbS CQD films.

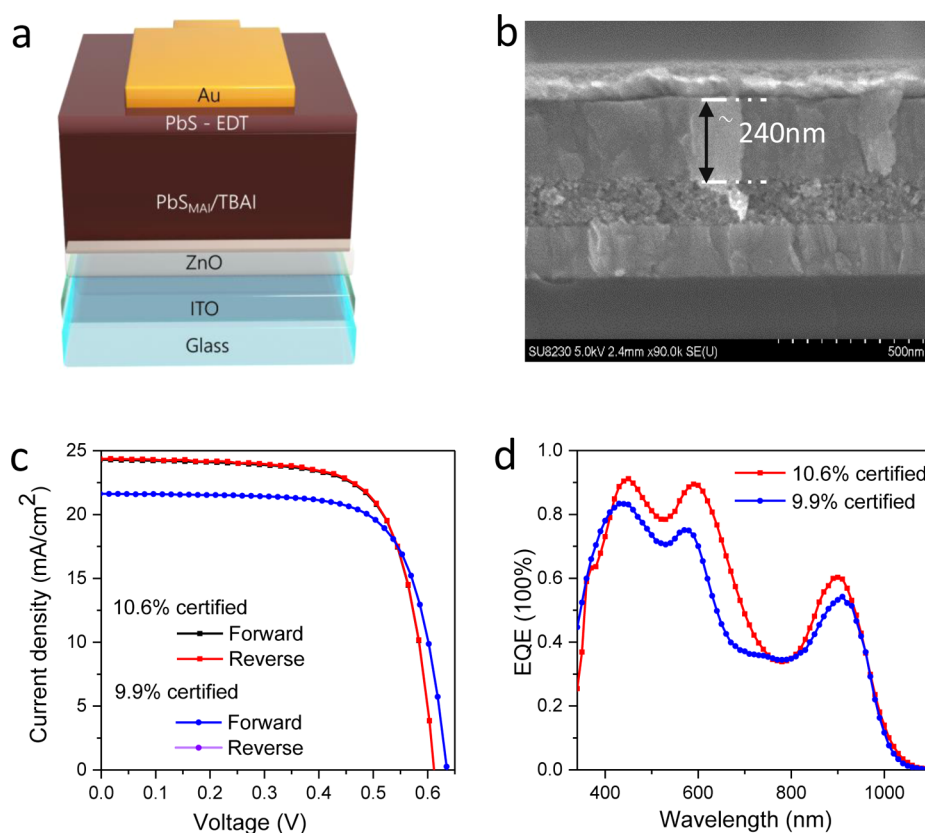


Figure 4. Device architecture and performance. (a) Schematic of the device architecture. (b) Cross-sectional SEM image of a 10.6% certified solar cell. (c) Hysteresis-free J - V characteristics and (d) the corresponding EQE of both 9.9% I_2 -pretreated and 10.6% MAI-pretreated certified solar cell devices.

MAI treatment (Figure 2c). Quantitative measurements by X-ray photoelectron spectroscopy (XPS), as shown in Figure 2d and Figure S4, show that the MAI solution pretreatment results in $\sim 20\%$ of OA displaced by iodine, which is three times higher than the ratio found from the previously reported I_2 treatment. The I_2 treatment resulted in fusion of PbS CQDs at similarly high I:Pb ratio. The improved iodine incorporation leads to enhanced passivation: following the MAI treatment, the PL quantum yield (QY) has increased to 29% from 15%, whereas the I_2 treatment achieves an increase to only 19%.

For the new MAI process, the CQDs are stable in the DMF-toluene treatment solution; however, once precipitated using

methanol and redispersed in octane, they are stable only for a few days. A long storage time will result in interdot fusion. Figure 3a shows the HRTEM image of 2-week aged CQDs following the MAI treatment. The PbS CQDs start to fuse and show a rectangular shape. This suggests that methanol washing process may remove the weakly bound ligand shell of $MA^+ - OA^-$ ion pairs participating in colloidal stabilization. NMR analysis of the methanol-washed CQDs shows that only surface-bound OA is maintained following methanol precipitation (Figure S5), consistent with the removal of the dynamically bound ligand shell.

We now show how the MAI treatment affects the final QD solid. Figure 3b shows the XPS analysis of the tetrabutylammonium iodide (TBAI)-exchanged PbS films. The results suggest that 43%, 47%, and 64% of the initial OA is replaced by iodide, for the untreated, I₂-treated and MAI-treated PbS CQD cases, respectively. This demonstrates that the MAI treatment does indeed lead to the highest iodide incorporation in the final film state.^{6,28} We hypothesize that surface sites can be occupied by other molecules, such as oxygen and water, during the film formation process. These molecules cannot repair the trap states that increase the recombination losses. With the MAI treatment, the preloading of iodide occupies these sites in the solution state, removing these electronic trap states and ultimately contributing to improved photovoltaic performance.

To show the advantages of the well-passivated PbS QDs, we constructed solar cells following the architecture shown in Figure 4a. Colloidal ZnO nanoparticles are coated on patterned ITO, which serve as the electron acceptor. This is followed by deposition of the two active layers, a thick layer of TBAI-exchanged PbS CQDs to be in direct contact with the ZnO, and an overlying thin layer of EDT-exchanged PbS CQDs. The MAI pretreatment results in partial removal of the oleate ligands. The remaining long-chain hydrophobic oleate ligands are crucial to maintain the colloidal stability of the CQDs in octane. For this reason, the solid-state ligand exchange process employing TBAI is required to assemble and densify the I-capped PbS CQD active region. After this process, all ammonium ligands are completely removed from the final films (Figure S4). Au electrodes are applied finally to afford ohmic contact. The enhanced passivation boosts photovoltaic performance: a certified efficiency of 10.6% was achieved (Figure S6). A cross-sectional SEM image of the device is shown in Figure 4b. The active layer thickness is ~240 nm, compared to 200 nm for control devices employing untreated CQDs.⁶ The increased thickness produces higher external quantum efficiency (EQE) and short-circuit current. Figure 4c shows the *J*-*V* curves from two certification runs (including 9.9% and 10.6%): notably, no hysteresis was observed during forward/reverse scanning. The V_{oc} , J_{sc} , and FF of the 10.6% certified device are 0.61 V, 24.3 mA/cm⁻², and 71%, respectively, compared to 0.63 V, 21.6 mA/cm⁻², and 72%, respectively, for the 9.9% certified device. The improvement comes mainly from the increase in J_{sc} . This is evidenced by a systematic increase in the external quantum efficiency (EQE) (Figure 4d). The EQE value at the exciton peak reaches 60%, indicating efficient charge extraction. This agrees with the view that improved passivation can contribute to enhanced diffusion lengths and thus enable thicker devices. We achieved a lab record efficiency of 10.8% with an even thicker device (~260 nm). The EQE and cross-sectional SEM image of the device are shown in Figure S7.

In summary, we present a new surface engineering approach that enables increased passivation using the iodide anion. The approach allows the ionic molecule, MAI, to access targeted nonpolar-dispersed CQDs by tuning the polarity of the dispersion medium. When we use this approach, we incorporate high amounts of iodide on CQDs to achieve improved passivation. The improved passivation facilitates the use of a thick photoactive layer in solar cell devices, delivering a certified efficiency of 10.6%. The method can be used more widely to engineer the surface chemistry of colloidal quantum dots, such as for stoichiometry tuning and surface doping.

■ ASSOCIATED CONTENT

Supporting Information

The Supporting Information is available free of charge on the ACS Publications website at DOI: 10.1021/acs.nanolett.6b01957.

Experimental details and other characterizations (PDF)

■ AUTHOR INFORMATION

Corresponding Author

*E-mail: ted.sargent@utoronto.ca.

Notes

The authors declare no competing financial interest.

■ ACKNOWLEDGMENTS

This publication is based in part on work supported by Award KUS-11-009-21, made by King Abdullah University of Science and Technology (KAUST), by the Ontario Research Fund - Research Excellence Program, and by the Natural Sciences and Engineering Research Council (NSERC) of Canada and by the International Cooperation of the Korea Institute of Energy Technology Evaluation and Planning (KETEP) grant funded by the Korea government Ministry of Knowledge Economy (2012T100100740). The authors thank E. Palmiano, R. Wolowiec, D. Kopilovic, R. Comin, R. Sabatini, X. Gong, J. Fan, and L. Levina, for their help over the course of this study.

■ REFERENCES

- (1) McDonald, S. A.; Konstantatos, G.; Zhang, S.; Cyr, P. W.; Klem, E. J.; Levina, L.; Sargent, E. H. *Nat. Mater.* **2005**, *4*, 138.
- (2) Chuang, C.-H. M.; Brown, P. R.; Bulović, V.; Bawendi, M. G. *Nat. Mater.* **2014**, *13*, 796.
- (3) Ip, A. H.; Thon, S. M.; Hoogland, S.; Voznyy, O.; Zhitomirsky, D.; Debnath, R.; Levina, L.; Rollny, L. R.; Carey, G. H.; Fischer, A.; Kemp, K. W.; Kramer, I. J.; Ning, Z.; Labelle, A. J.; Chou, K. W.; Amassian, A.; Sargent, E. H. *Nat. Nanotechnol.* **2012**, *7*, 577.
- (4) Semonin, O. E.; Luther, J. M.; Choi, S.; Chen, H.-Y.; Gao, J.; Nozik, A. J.; Beard, M. C. *Science* **2011**, *334*, 1530.
- (5) Kamat, P. V. *J. Phys. Chem. C* **2008**, *112*, 18737.
- (6) Lan, X.; Voznyy, O.; Kiani, A.; García de Arquer, F. P.; Abbas, A. S.; Kim, G.-H.; Liu, M.; Yang, Z.; Walters, G.; Xu, J.; Yuan, M.; Ning, Z.; Fan, F.; Kanjanaboos, P.; Kramer, I.; Zhitomirsky, D.; Lee, P.; Perelgut, A.; Hoogland, S.; Sargent, E. H. *Adv. Mater.* **2016**, *28*, 299.
- (7) Polman, A.; Knight, M.; Garnett, E. C.; Ehrler, B.; Sinke, W. C. *Science* **2016**, *352*, 307.
- (8) McGuire, J. A.; Joo, J.; Pietryga, J. M.; Schaller, R. D.; Klimov, V. I. *Acc. Chem. Res.* **2008**, *41*, 1810.
- (9) Tang, J.; Kemp, K. W.; Hoogland, S.; Jeong, K. S.; Liu, H.; Levina, L.; Furukawa, M.; Wang, X.; Debnath, R.; Cha, D.; Chou, K. W.; Fischer, A.; Amassian, A.; Asbury, J. B.; Sargent, E. H. *Nat. Mater.* **2011**, *10*, 765.
- (10) Mathew, S.; Yella, A.; Gao, P.; Humphry-Baker, R.; Curchod, B. F.; Ashari-Astani, N.; Tavernelli, I.; Rothlisberger, U.; Nazeeruddin, M. K.; Grätzel, M. *Nat. Chem.* **2014**, *6*, 242.
- (11) You, J.; Dou, L.; Yoshimura, K.; Kato, T.; Ohya, K.; Moriarty, T.; Emery, K.; Chen, C.-C.; Gao, J.; Li, G.; Yang, Y. *Nat. Commun.* **2013**, *4*, 1446.
- (12) Hines, M. A.; Scholes, G. D. *Adv. Mater.* **2003**, *15*, 1844.
- (13) Peng, X.; Manna, L.; Yang, W.; Wickham, J.; Scher, E.; Kadavanich, A.; Alivisatos, A. P. *Nature* **2000**, *404*, 59.
- (14) Peng, Z. A.; Peng, X. *J. Am. Chem. Soc.* **2001**, *123*, 1389.
- (15) Hendricks, M. P.; Campos, M. P.; Cleveland, G. T.; Jen-La Plante, I.; Owen, J. S. *Science* **2015**, *348*, 1226.
- (16) Alivisatos, A. P. *Science* **1996**, *271*, 933.
- (17) Scheele, M.; Engel, J. H.; Ferry, V. E.; Hanifi, D.; Liu, Y.; Alivisatos, A. P. *ACS Nano* **2013**, *7*, 6774.

- (18) Sandeep, C. S.; Azpiroz, J. M.; Evers, W. H.; Boehme, S. C.; Moreels, I.; Kinge, S.; Siebbeles, L. D.; Infante, I.; Houtepen, A. J. *ACS Nano* **2014**, *8*, 11499.
- (19) Carey, G. H.; Levina, L.; Comin, R.; Voznyy, O.; Sargent, E. H. *Adv. Mater.* **2015**, *27*, 3325.
- (20) Liu, W.; Lee, J.-S.; Talapin, D. V. *J. Am. Chem. Soc.* **2013**, *135*, 1349.
- (21) Law, M.; Luther, J. M.; Song, Q.; Hughes, B. K.; Perkins, C. L.; Nozik, A. J. *J. Am. Chem. Soc.* **2008**, *130*, 5974.
- (22) Liu, Y.; Gibbs, M.; Puthussery, J.; Gaik, S.; Ihly, R.; Hillhouse, H. W.; Law, M. *Nano Lett.* **2010**, *10*, 1960.
- (23) Whitham, K.; Yang, J.; Savitzky, B. H.; Kourkoutis, L. F.; Wise, F.; Hanrath, T. *Nat. Mater.* **2016**, *15*, 557.
- (24) Yang, Z.; Janmohamed, A.; Lan, X.; García de Arquer, F. P.; Voznyy, O.; Yassitepe, E.; Kim, G.-H.; Ning, Z.; Gong, X.; Comin, R.; Sargent, E. H. *Nano Lett.* **2015**, *15*, 7539.
- (25) Choi, J.-H.; Fafarman, A. T.; Oh, S. J.; Ko, D.-K.; Kim, D. K.; Diroll, B. T.; Muramoto, S.; Gillen, J. G.; Murray, C. B.; Kagan, C. R. *Nano Lett.* **2012**, *12*, 2631.
- (26) Kovalenko, M. V.; Scheele, M.; Talapin, D. V. *Science* **2009**, *324*, 1417.
- (27) Zhang, H.; Jang, J.; Liu, W.; Talapin, D. V. *ACS Nano* **2014**, *8*, 7359.
- (28) Ning, Z.; Voznyy, O.; Pan, J.; Hoogland, S.; Adinolfi, V.; Xu, J.; Li, M.; Kirmani, A. R.; Sun, J.-P.; Minor, J.; Kemp, K. W.; Dong, H.; Rollny, L.; Labelle, A.; Carey, G.; Sutherland, B.; Hill, I.; Amassian, A.; Liu, H.; Tang, J.; Bakr, O. M.; Sargent, E. H. *Nat. Mater.* **2014**, *13*, 822.
- (29) Zhang, J.; Gao, J.; Church, C. P.; Miller, E. M.; Luther, J. M.; Klimov, V. I.; Beard, M. C. *Nano Lett.* **2014**, *14*, 6010.
- (30) Crisp, R. W.; Kroupa, D. M.; Marshall, A. R.; Miller, E. M.; Zhang, J.; Beard, M. C.; Luther, J. M. *Sci. Rep.* **2015**, *5*, 9945.
- (31) Anderson, N. C.; Hendricks, M. P.; Choi, J. J.; Owen, J. S. *J. Am. Chem. Soc.* **2013**, *135*, 18536.
- (32) Doris, S. E.; Lynch, J. J.; Li, C.; Wills, A. W.; Urban, J. J.; Helms, B. A. *J. Am. Chem. Soc.* **2014**, *136*, 15702.
- (33) De Roo, J.; Ibáñez, M.; Geiregat, P.; Nedelcu, G.; Walravens, W.; Maes, J.; Martins, J. C.; Van Driessche, I.; Kovalenko, M. V.; Hens, Z. *ACS Nano* **2016**, *10*, 2071.